Vehicular Low-Profile Dual-Band Antenna for Advanced Tyre Monitoring Systems

Gregor Lasser and Christoph F. Mecklenbräuker*
Vienna University of Technology
Institute of Telecommunications
Gusshausstrasse 25/389, 1040 Vienna, Austria
Email: gregor.lasser@nt.tuwien.ac.at
*Christian Doppler Laboratory for Wireless Technologies for Sustainable Mobility

***Abstract*—In this contribution we design, implement and characterise a novel low-profile dual-band loop antenna suitable for advanced tyre monitoring systems by measurements. The antenna is omnidirectional in azimuth, vertically polarised and suited for the European UHF and microwave RFID bands. Our proposed antenna is compared to a modified monopole antenna, which is in resonance at the same bands. Both antennas were manufactured and afterwards measured in an anechoic chamber. Directional patterns and measured antenna efficiencies are presented.**

I. Introduction

Tyre pressure monitoring systems have become standard components of most modern personal vehicles. This success is also promoted by legislation and aims to increase vehicular safety and lower fuel consumption by ensuring proper tyre inflation. Current direct tyre pressure monitoring systems use rather bulky sensor units mounted at the rim of the wheel and use batteries to supply the sensor electronics and a transmitter circuit. By moving the sensor unit to the tyre itself, more parameters can be sensed and tyre identification is possible. These systems are called Advanced Tyre Monitoring Systems (ATMS) [1]. Due to the volume and weight constraints involved with this mounting position, the sensor units have to be very small and preferably omit a battery for power supply. A possible candidate for communications therefore is passive Radio Frequency Identification (RFID) technology which relies on power efficient backscattering technology and to use radio frequency energy harvesting to power the sensor circuitry.

Feasibility to include RFID tags in truck tyres was shown in [2] and tyres with embedded RFID tags are now also available commercially [3]. However, in both cases the RFID tags are not read during vehicle movement as necessary for ATMS and proposed by [4]. For this approach, knowlege about the radio channel between the sensor unit and a receiver antenna mounted on the vehicle is crucial [5]–[7], so that read probabilities can be estimated [8].

In this paper we will present a novel low-profile dual-band antenna suitable for vehicular body floor pan mounting. We will compare this antenna to a modified monopole antenna which was used for the static channel measurements described in [7] which is unhandy for practical use due to its physical dimensions. Both antennas serve the European UHF RFID band at 865 MHz to 868 MHz as well as the 2.45 GHz ISM band.

This work has been funded by the Christian Doppler Laboratory for Wireless Technologies for Sustainable Mobility.

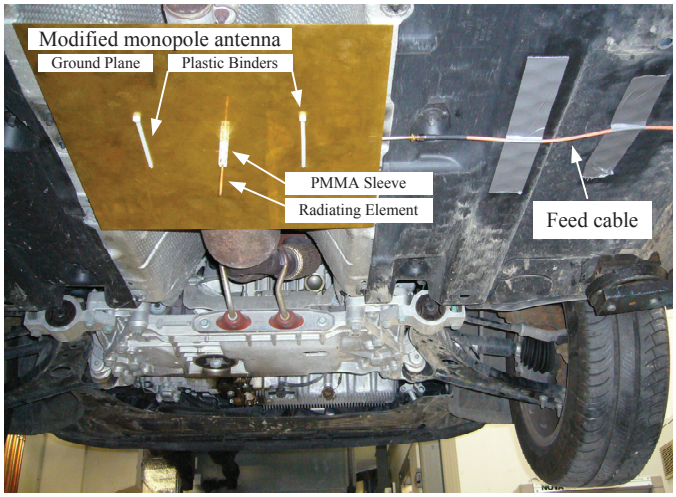

Fig. 1. Image of the modified monopole antenna mounted to vehicle body floor pan in preparations for channel measurements [7].

II. Monopole Antenna

In this section we present a modified monopole antenna which was designed for the dual-band channel measurements presented in [7], but there the antenna itself was barely discussed. The design goals of this antenna are high efficiency, low influence from the uneven vehicular body floor pan, simple construction and dual-band capabilities at both, the European UHF (865 MHz to 868 MHz) and the microwave RFID band at 2.4 GHz to 2.5 GHz. Additionally, a low elevation angle is preferable, to beam the main lobe of the antenna towards the wheels.

Fig. 2 presents a technical drawing of the monopole antenna, its mechanical parameters are summarized in Table I. To reduce the effects of the uneven vehicular body floor pan and ensure a low elevation angle, a rather large groundplane

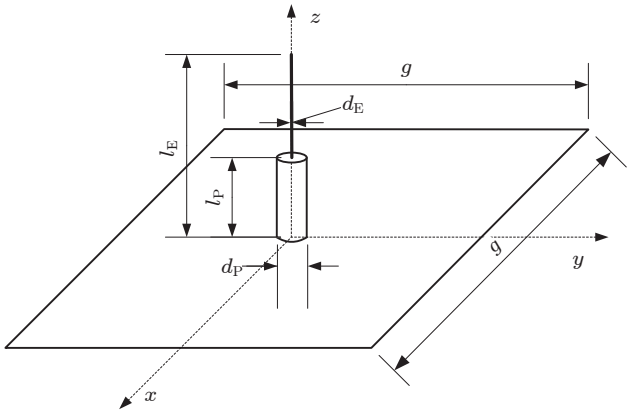

Fig. 2. Dimensional drawing of the modified monopole antenna.

TABLE I
MECHANICAL PARAMETERS OF MODIFIED MONOPOLE ANTENNA.

Geometry Parameter	Variable	Value	Unit
Groundplane	g	40×40	cm
Element length	l_E	78	mm
Element diameter	d_E	3	mm
PMMA cylinder length	l_P	34	mm
PMMA cylinder diameter	d_P	10	mm

with dimensions of 1.16 wavelengths λ manufactured from brass is used. The radiating element located in the center of the groundplane is comprised of a copper tube with an outer diameter of $d_E = 3\,\mathrm{mm}$. The radiating element is directly fed through a hole in the groundplane with a semi-rigid coaxial cable of the RG–402 variety, which is terminated in a female SMA connector. The outer conductor of the coaxial feed cable is soldered to the backside of the groundplane over the entire length to form an electrically and mechanically sound connection. This conventional monopole antenna was modified by placing a dielectric sleeve constructed from polymethylmethacrylate (PMMA) on the lower part of the radiating element. This dielectric loading electrically lengthens the radiating element, especially in regions bearing large electric fields. Due to the well known voltage distribution along a monopole this dielectric loading close to the groundplane does not severely affect the $\lambda/4-$resonance of the monopole. However, the third harmonic is strongly affected due to the location of one voltage peak on the radiating element close to the groundplane for $3\lambda/4-$resonance. Based on this concept, the PMMA sleeve allows shifting of the natural third harmonic resonance at 2.600 GHz down to 2.45 GHz.

A. Simulation Results and Return Loss Measurements

Prior to actual implementation of the antenna the authors conducted simulations in Ansoft's HFSS electromagnetic field simulatior. The permittivity of of the PMMA cylinder was set to $\varepsilon_r = 2.6$ and its loss tangent was set to $\tan\delta = 0.008$, based on the results of [9], which were measured at 10 GHz. After fabrication of the antenna and measurement of the return loss with a vector network analyser (VNA), the dielectric cylinder

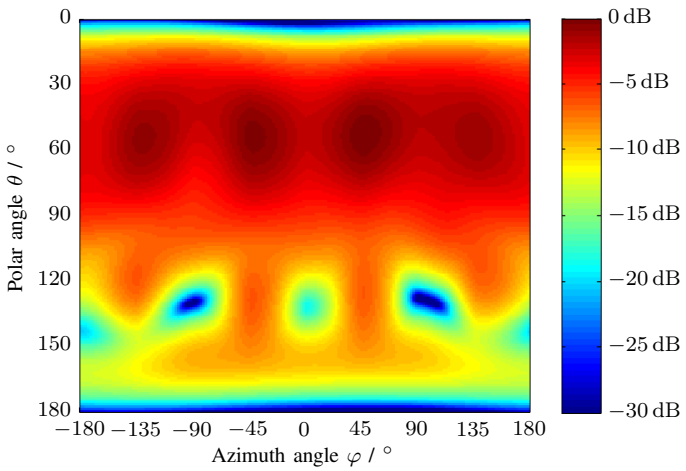

Fig. 3. Logarithmically scaled pseudo-color plot of the gain pattern of the modified monopole antenna at 866 MHz for vertical polarisation.

proofed to be slightly too long, which was caused by underestimation of the permittivity of the PMMA at 2.45 GHz, and so it was shortened to the length stated in Table I. The simulation was adapted by performing a parameter sweep of the dielectric constant of the PMMA cylinder using the actual antenna geometry parameters and picking the permittivity value of $\varepsilon_r = 3$ where simulated and measured return loss peaks of the $3\lambda/4-$resonance coincide in frequency. A comparison between the resulting simulated an measured return losses is plotted in Fig. 10. The antenna achieves a very good return loss of better than 14 dB from 856 MHz to 885 MHz and has an acceptable return loss of 8 dB from 2.4 GHz to 2.5 GHz.

The simulated radiation efficiency including material losses is found to be 99 % at the lower band and 100 % at 2.45 GHz. By including the matching losses the overall efficiency is calculated to be 93 % and 86 % at 2.45 GHz, respectively.

B. Anechoic Chamber Measurement Results

The antenna is placed in our anechoic chamber and a near field measurement is performed. The near field data is transformed to far field data and probe correction for the used dual ridged horn is applied. A pseudo-colour plot of the antenna pattern is shown in Fig. 3. This plot, as well as all following pattern plots is normalised to the global peak of the antenna being $1 = 0\,\mathrm{dB}$. The antenna exhibits an almost omnidirectional pattern in azimuth, as is expected for a monopole antenna. However, due to the square shaped groundplane, four lobes pointing in the direction of the edges of the groundplane appear, which are also identified in the azimuth radiation pattern in Fig. 4. If the antenna is mounted almost flush with the vehicle body floor pan as presented in Fig. 1, we expect this effect to be minimised due to the additional extension of the groundplane by the metallic environment. However, when mounting the antenna slightly lower, this beam-effect can be utilised by shaping the groundplane according to the tyre and reader antenna positions.

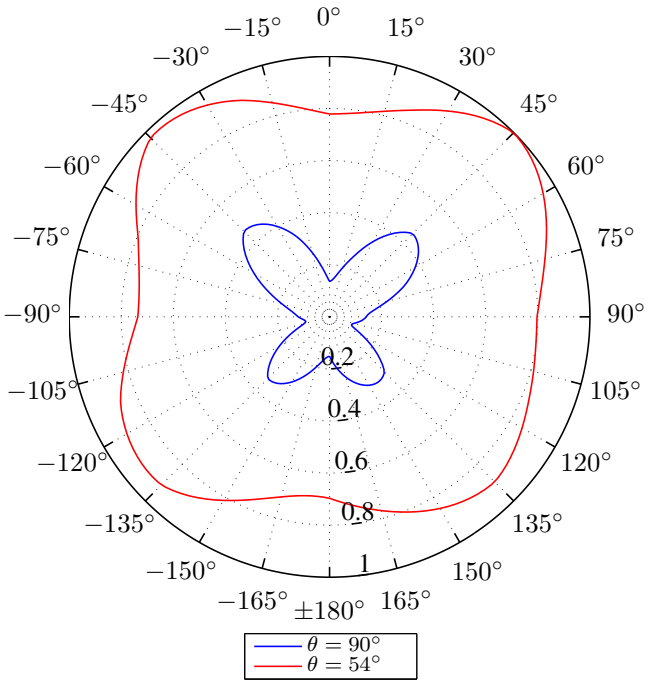

Fig. 4. Radiation pattern of the modified monopole antenna in Azimuth at 866 MHz.

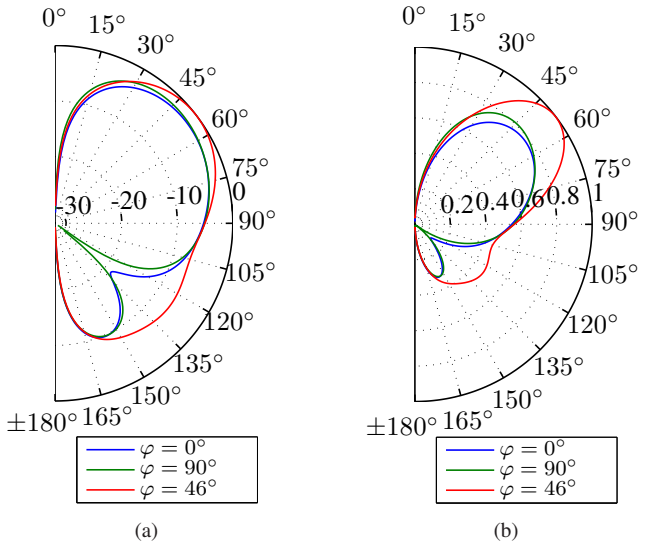

Fig. 5. Radiation pattern of the modified monopole antenna in polar angle at 866 MHz, plotted logarithmically (a) and linear (b) for three φ-cuts.

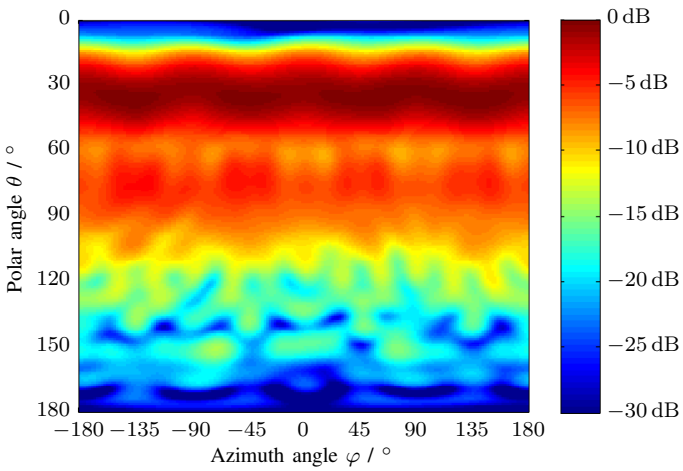

Fig. 6. Logarithmically scaled pseudo-color plot of the gain pattern of the modified monopole antenna at 2.45 GHz for vertical polarisation.

An additional noticeable effect is a slight concentration of the radiated energy towards small azimuth angles. This is caused by the coaxial feed cable which is protruding from the groundplane on the x-axis, acting as a counterpoise for the radiating element similar like the corners of the groundplane. Again, this effect will be minimised in mounting scenarios similar to Fig. 1.

The azimuth radiation pattern Fig. 4 is plotted for $\theta = 90°$ and $\theta = 54°$ as this is the polar angle of the main lobe. The dependency on the polar angle is plotted in Fig. 5. For all azimuth angles the main beam elevation angle stays almost constant at 36°, but the beam is relatively broad in elevation so that for zero elevation ($\theta = 90°$) the power is reduced by only 5 dB. The directivity calculated from the measurement results is found to be 4.3 dB.

At 2.45 GHz the the elevation angle gets higher, but a sidelobe at a low elevation angle of 15° appears, which can be seen both in the pseudo-colour plot Fig. 6 and the polar plot Fig. 7. Due to the smaller wavelength, the groundplane is electrically about three times larger than for the lower band, and therefore only minor power concentration towards the groundplane edges is noticable in Fig. 6. Compared to the lower frequency pattern, radiated power is more concentrated in θ and the directivity at 2.45 GHz is 6.7 dB.

III. Low Profile Dual-band Loop

While the modified monopole presented before is an electrically perfect solution for an omnidirectional vehicular body floor pan antenna for ATMS, it is unsuitable for practical implementation due to its mechanical dimensions. A well known candidate for a vertical polarised omnidirectional antenna is the Directly Driven Resonant Radiator (DDRR) antenna described in [10], [11]. The antenna principle of the DDRR antenna is based on a very short vertical radiator, which is top-loaded with a loop shaped transmission line to achieve impedance matching. While in both publications, the end of the transmission line is terminated in a tuning capacitor, our approach is to omit this capacitor similar to [12]. In contrast to the mentioned authors, the proposed Low Profile Dual-band Loop (LPDL) is tuned at two operational frequencies simultaneously by a capacity coupled shortening structure in the loop center.

The proposed LPDL antenna, as shown in Fig. 8, has the same brass groundplane dimensions as the modified monopole antenna, but its height is dramatically reduced to 6.5 mm. The vertical radiator is directly constructed from the center conductor of the feeding coaxial cable, which is a silver plated

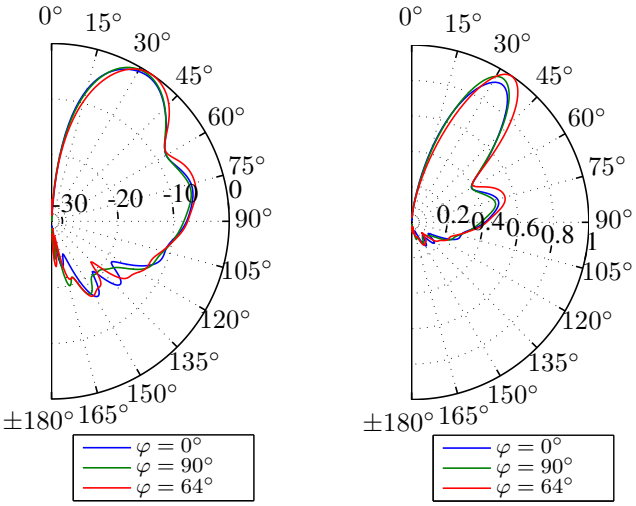

Fig. 7. Radiation pattern of the modified monopole antenna in polar angle at 2.45 GHz, plotted logarithmically (a) and linear (b) for three φ-cuts.

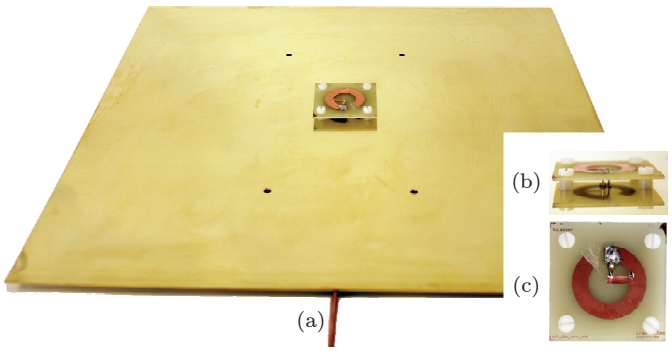

Fig. 8. Image showing the LPDL antenna (a), and close-ups of the vertical feed (b), and the PCB (c).

steel wire. The resonant loop structure is manufactured as copper trace on a single–sided FR–4 Printed Circuit Board (PCB). This PCB is mounted 5 mm above the groundplane using four screws and spacers, both manufactured from Nylon. Adding the PCB thickness of 1.5 mm the loop is elevated 6.5 mm ($\approx 0.019\,\lambda$) above the groundplane. The vertical radiator is soldered to the copper trace on top of the PCB, as well as three silver plated copper wires which serve as ground connection for the resonator. This feeding is similar to an inverted–F antenna, except that the stub of the inverted–F is coiled up in a loop. Details are given in Fig. 9 and Table II. To reach resonance at 2.45 GHz, an additional shortening structure inside the loop is used, which is coupled to the feed by means of a small variable capacitor C. This capacitor is adjustable between 0.55 pF and 1 pF and was tuned for best matching at 2.45 GHz by means of a VNA.

A. Simulation Results and Measured Return Loss

The LPDL antenna was again simulated in HFSS. This time, the after some optimisations using the VNA the actual geometry as described in Table II was entered into the simulation

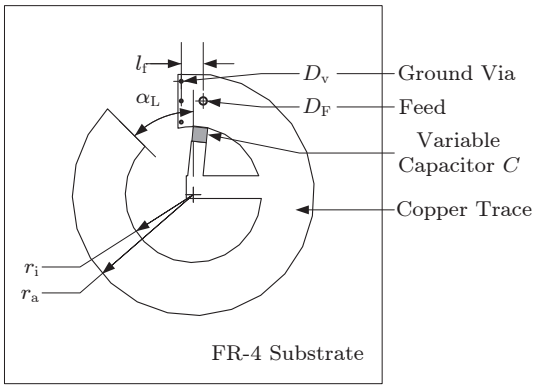

Fig. 9. Dimensional drawing of the LPDL antenna PCB on a scale of 1:1.

TABLE II
MECHANICAL PARAMETERS OF LPDL ANTENNA.

Geometry Parameter	variable	Value	Unit
Groundplane	g	40×40	cm
FR-4 Substrate dimensions		$50 \times 50 \times 1.5$	mm
Substrate–groundplane seperation	h	5	mm
Feed distance	l_f	2.8	mm
Feed diameter	D_F	0.9	mm
Ground via diameter	D_v	0.5	mm
Inner loop radius	r_i	9	mm
Outer loop radius	r_a	16	mm
Loop opening angle	α_L	45°	

environment and a parameter sweep over the capacitance C was conducted. Best agreement at the 2.45 GHz resonance peak was found for $C = 0.6$ pF, this result is also depicted in Fig. 10. The agreement at the lower frequency resonance is not perfect, which is most likely caused by the permittivity of the PCB material, which is not well defined for FR–4.

Both, measured and simulated antenna return losses of the LPDL presented in Fig. 10 show the typical drawback of resonant structures — their bandwidth is small if the losses are not dominating. However, measurements of the return loss of the manufactured LPDL antenna show that the RFID band is still very well matched, in fact the 10 dB bandwidth ranges from 861 MHz to 869 MHz. For actual vehicular implementation the antenna has to be covered in a radome to prevent detuning caused by accumulations of dirt.

The measured matching at the upper band is slightly degraded, when compared to the simulations and the measured 6 dB return loss bandwidth is ranging from 2.42 GHz to 2.49 GHz. The authors believe that by small geometrical changes to the shortening structure inside the loop this matching can be further improved.

B. Anechoic Chamber Measurement Results

The LPDL antenna was measured in the same test range and directly after the modified monopole antenna to enable direct comparison and relative efficiency measurements. The overall relative efficiency of the LPDL antenna including matching losses, when compared to the modified monopole, was found

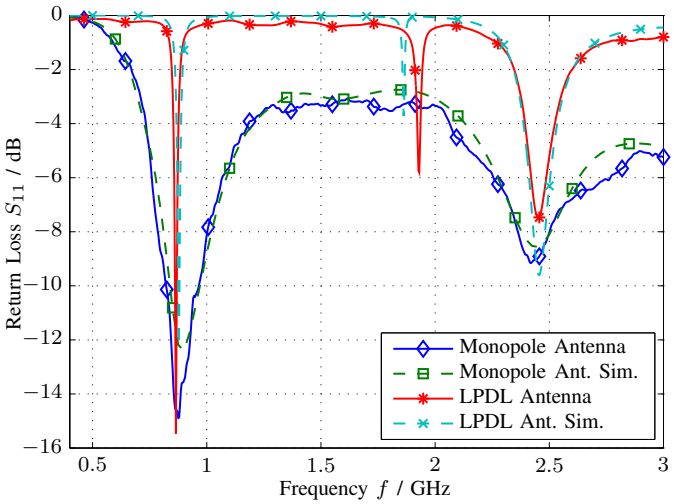

Fig. 10. Comparison of antenna return losses of both antennas, both measured and simulated.

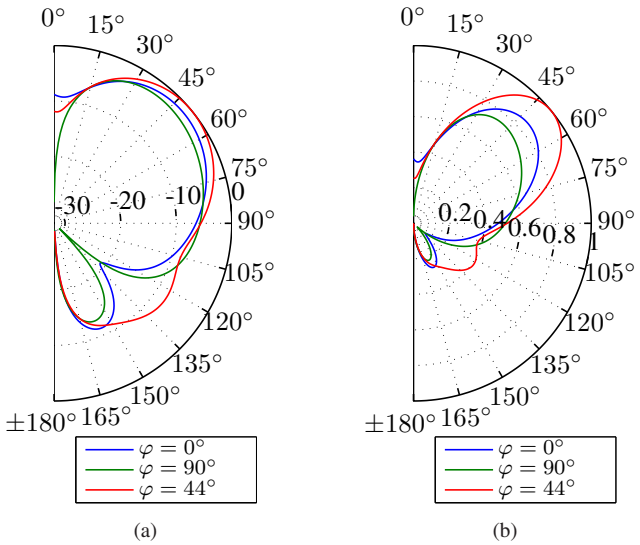

Fig. 12. Radiation pattern of the LPDL antenna in polar angle at 866 MHz, plotted logarithmically (a) and linear (b) for three φ-cuts.

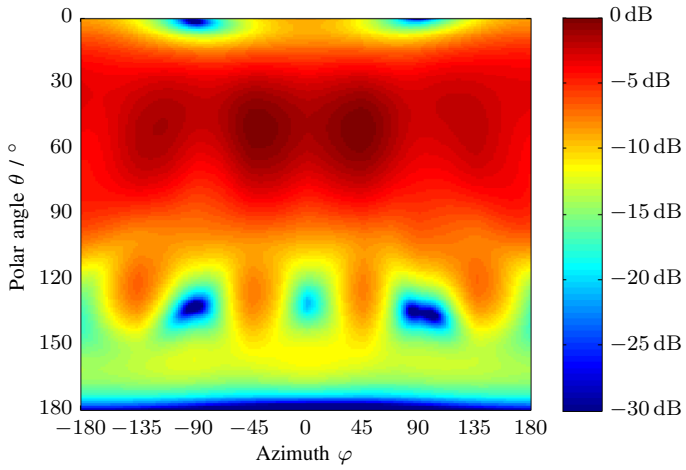

Fig. 11. Logarithmically scaled pseudo-color plot of the gain pattern of the LPDL antenna at 866 MHz for vertical polarisation.

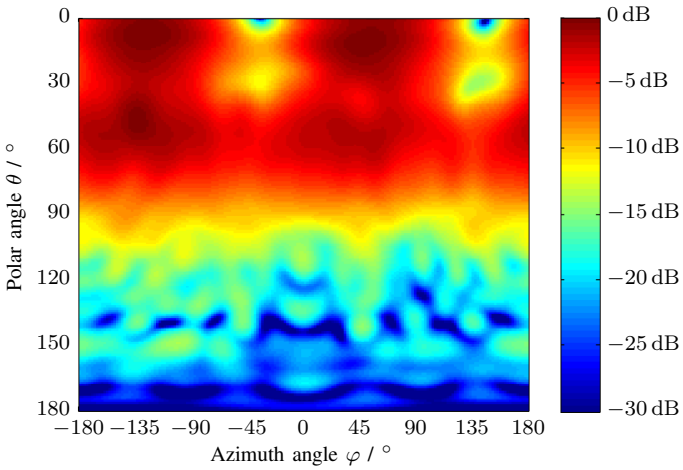

Fig. 13. Logarithmically scaled pseudo-color plot of the gain pattern of the LPDL antenna at 2.45 GHz for vertical polarisation.

to be 37 % in the UHF band and 68 % at the 2.45 GHz microwave band.

The radiation pattern at 866 MHz is shown in the pseudo–colour plot in Fig. 11. Despite the dramatically shortened vertical radiator the radiation pattern looks very similar to the one of the resonant monopole depicted in Fig. 3. The same is true for the dependency in the polar angle θ, when Fig. 12 and Fig. 5 are compared. Therefore, it is not surprising that the directivity of the LPDL is also very similar to the monopole, the measured value is 4.6 dB. The elevation angle is slightly increased to 39°, but at $\theta = 90°$ the radiation intensity is still 5 dB down.

At the upper band the antenna parameters change more significantly, because parts of the loop act as a horizontal radiator. Fig. 13 and Fig. 14(b) show a forked beam in θ, with one part being elevated 83° ($\theta = 7°$) and a second one at at $\theta = 48°$ corresponding to an elevation of 42°. While the first part is not very beneficial for the proposed vehicular ATMS application, the second lobe has a lower elevation than the main lobe of the modified monopole, as depicted in Fig. 7. According to Fig. 14(a) the high elevated beam at $\theta = 7°$ shows an almost dipole-like radiation pattern which is caused by the radiation of the inner shortening structure of the LPDL. While the weak beam at $\theta = 90°$ is almost perfectly omnidirectional, the slightly elevated beam beneficial for the proposed ATMS application is slightly elliptically shaped. The directivity calculated from the measurement results at this operation frequency is 5.5 dB and therefore slightly lower than the one of the monopole which does not show the forked beams.

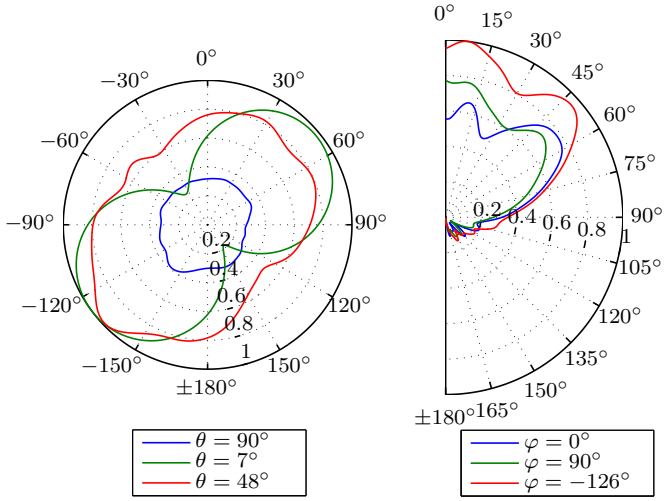

(a) (b)

Fig. 14. Linear radiation pattern of the modified monopole antenna at 2.45 GHz, plotted over azimuth φ (a) and over polar angle θ (b) for three cuts.

IV. Conclusion

Tyre pressure monitoring systems have become state-of-the-art and are now being widely deployed for fighting fuel consumption and for enhancing traffic safety. ATMS, the evolution towards tyre embedded sensors is currently under investigation. Power transfer and communications require efficient, but low-profile antennas, suitable for vehicular body floor pan mounting.

In this contribution we present a novel low profile dual-band loop (LPDL) antenna suitable for this application, operating at the UHF 866 MHz and microwave 2.45 GHz RFID bands. It is an omnidirectional, vertically polarised antenna with a low elevation angle. The antenna is compared to a modified monopole antenna which has similar radiation patterns.

Both antennas were manufactured and measured in an anechoic chamber and simulation and measurement results are presented. Despite its size of 8.3 % of the monopole antenna, the proposed LPDL antenna shows overall relative efficiencies of 37 % in the UHF band and 68 % at the 2.45 GHz microwave band when compared to the resonant monopole. While the radiation pattern at 866 MHz is very similar to the monopole and a directivity of 4.6 dB is achieved, the radiation pattern at 2.45 GHz shows a lower elevation angle, which is beneficial for ATMS application.

References

[1] S. C. Ergen, A. Sangiovanni-Vincentelli, X. Sun, R. Tebano, S. Alalusi, G. Audisio, and M. Sabatini, "The tire as an intelligent sensor," *IEEE Trans. Comput.-Aided Design Integr. Circuits Syst.*, vol. 28, pp. 941–955, Jul. 2009.

[2] L. Kovavisaruch, P. Lertudomtana, and S. Horungruang, "Management truck tire information in logistic industry using RFID technology," in *Management of Engineering Technology, 2008. PICMET 2008. Portland International Conference on*, Jul. 2008, pp. 1656 –1665.

[3] Goodyear Dunlop Tires Europe B.V., "Goodyear markets first microchipped truck tires," *Goodyear News*, Nov. 2011.

[4] H. J. Kulka, J. H. Schramm, and A. Arbor, "Active integrated circuit transponder and sensor apparatus for sensing and transmitting vehicle tire parameter data," U.S. Patent, Jan. 16, 1996.

[5] H. J. Song, J. S.Colburn, H. P. Hsu, and R. W. Wiese, "Development of reduced order model for modeling performance of tire pressure monitoring system," *Vehicular Technology Conference, 2006. VTC-2006 Fall. IEEE 64th*, pp. 1–5, Sep. 2006.

[6] M. Brzeska and G.-A. Chakam, "RF modelling and characterization of a tyre pressure monitoring system," *The Second European Conference on Antennas and Propagation, 2007. EuCAP*, pp. 1–6, Nov. 2007.

[7] G. Lasser and C. F. Mecklenbräuker, "Dual-band channel measurements for an advanced tyre monitoring system," *Vehicular Technology Conference. VTC 2010-Spring. IEEE 71th*, pp. 1–5, May 2010.

[8] G. Lasser, R. Langwieser, F. Xaver, and C. F. Mecklenbräuker, "Dual-band channel gain statistics for dual-antenna tyre pressure monitoring RFID tags," in *Proceedings of the 2011 IEEE International Conference on RFID*. Orlando, Fl: IEEE, Apr. 2011, pp. 57–61.

[9] B. Riddle, J. Baker-Jarvis, and J. Krupka, "Complex permittivity measurements of common plastics over variable temperatures," *IEEE Trans. Microw. Theory Tech.*, vol. 51, no. 3, pp. 727 – 733, Mar. 2003.

[10] J. M. Boyer, "Open ring antenna," U.S. Patent, Sep. 29, 1964.

[11] R. D. Wanselow and D. W. Milligan, "A compact, low profile, transmission line antenna — tuneable over greater than octave bandwidth," *IEEE Trans. Antennas Propag.*, vol. AP-14, no. 6, pp. 701 – 707, Nov. 1966.

[12] A. M. Smith, "Vandalism-resistant UHF antenna," U.S. Patent, Apr. 28, 1987.